Proceedings of IDETC/CIE 2005
ASME 2005 International Design Engineering Technical Conferences
& Computers and Information in Engineering Conference
September 24-28, 2005, Long Beach, California USA

DETC2005-84349

HYBRID TARGET TRACKING MANIPULATION THEORIES FOR COMBINED FORCE AND POSITION CONTROL IN OPEN AND CLOSED LOOP MANIPULATORS

David J. Giblin
Graduate Student
Department of Mechanical Engineering
University of Connecticut
Storrs, CT - 06269
dgiblin@engr.uconn.edu

Mu Zongliang
Graduate Student
Department of Mechanical Engineering
University of Connecticut
Storrs, CT - 06269
z.mu@genaissance.com

ZhongXue Gan
Manager
Robotics Technology
ABB
Windsor, CT – 06095
zhongxue.gan@us.abb.com

Kazem Kazerounian
Professor and Fellow of ASME
Department of Mechanical Engineering
University of Connecticut
Storrs, CT - 06269
kazem@engr.uconn.edu

ABSTRACT

This paper presents a new manipulation theory for controlling compliant motions of a robotic manipulator. In previous closed loop control methods, both direct kinematics and inverse kinematics of a manipulator must be resolved to convert feedback force and position data from Cartesian space to joint space. However, in many cases, the solution of direct kinematics in a parallel manipulator or the solution of inverse kinematics in a serial manipulator is not easily available. In this study, the force and position data are packed into one set of "motion feedback," by replacing the force errors with virtual motion quantities, or one set of "force feedback," by replacing motion errors with virtual force quantities. The joint torques are adjusted based on this combined feed back package. Since only Jacobian of direct kinematics or Jacobian of inverse kinematics is used in the control scheme, the computational complexity is reduced significantly. The applications of this theory are demonstrated in simulation experiments with both serial and parallel manipulators.

KEYWORDS

Target tracking, open loop, closed loop, manipulation, hybrid control

INTRODUCTION

In many applications such as deburring, grinding, scribing and contour following, a manipulator is required to follow a predefined position trajectory in the tangent direction of a surface while maintaining a contact force in the normal direction. These tasks need appropriate control of motion and force.

In the beginning, a typical force control strategy was used to command an actuator torque. This strategy combined feedback of force with feedback of position (and velocity) and corrected the error through a common controller [1,2]. In 1981, Raibert and Craig proposed a conceptually simple method, which is currently referred as Hybrid Control [3]. This method employs a selection matrix that separates force and position errors and adopts independent controllers for each. This scheme avoided the unnecessary burden of "correction cycles" introduced by the interference between position errors and force errors. This was followed and improved upon by many researchers [4,5]. Sources of "kinematic instability" were identified and corrected in Raibert and Craig's method [6,7,8]. Fisher and Mujtaba documented some sufficient conditions for kinematic stability in hybrid control. A contact model was developed using projection matrices to decompose force and motion vectors that extended the Raibert Craig model to more general tasks, such as intricate two-point contact models [9].

In 1985, Hogan proposed a generalized impedance control scheme targeted at controlling a dynamic relation between the manipulator and its environment [10,11,12]. It controls the manipulator's motion and compensates with a responsive actuator torque to deviations from that motion which has the form of impedance. Subsequently reported studies of impedance control have focused on practical and implementation issues [13,14,15,16]. Walker utilized kinematic redundancy to alleviate impact problems in manipulator control [17]. The effectiveness of his approach depends on the manipulator configuration.

In previous studies, the kinematic solution of a manipulator is an important part in the control cycle. For hybrid control of force and position, both solutions of forward and reverse kinematics of a manipulator are often needed or at least an inversion of the system Jacobian is part of the calculation. This paper investigates a computationally efficient manipulation theory which stems from target tracking method developed by Kazerounian and Gupta [18].

In the following sections, the formulation of the target tracking theory is introduced and two simulation experiments are given to demonstrate its applications on a serial manipulator and parallel manipulator.

NOMENCLATURE

J —System Jacobian
$\mathbf{J}^{-1}$ —Inverse Jacobian
$\mathbf{J}^{T}$ —Transpose Jacobian
G —Gravity
X—Position and orientation of end-effector
F — external force and moment applied on the end-effector
τ — Joint torques
q — Joint values
S —Selection matrix
I —Identity matrix
K_I, K_d, K_p—Integral, differential and proportional gains
H—end-effector (hand)
θ, Φ, Ψ —XYZ Euler
Coordinate system $O_m(X_m\text{-}Y_m\text{-}Z_m)$ –Coordinate system rigid to the end effector
Coordinate system $O_n(X_n\text{-}Y_n\text{-}Z_n)$ –Coordinate system rigid to ground

Conventions followed:

Bold letters indicate matrices or vectors.
Plain letters indicate scalars or constants.
Superscript ^{d} indicates desired values.
Superscript ^{a} indicates actual values.
Superscript ^{M} indicates quantities in end-effector coordinate system $O_m(X_m\text{-}Y_m\text{-}Z_m)$.
Superscript ^{N} indicates quantities in global coordinate system $O_n(X_n\text{-}Y_n\text{-}Z_n)$.
Quantities are in O_m system if not indicated explicitly.
Subscript $_e$ indicates errors.
All length and position are in unit of Meter(m) .
All angular values are in radians.
Forces and torques are in unit of Newton(N) and Newton·Meter (Nm), respectively.

TARGET TRACKING THEORY COMBINING FORCE AND POSITION CONTROL

For compliant motion, a manipulator moves its hand along a generalized surface in a task space of N-DOF. It has position constraints along the normal directions and force constraints along the tangent directions. Correspondingly, the forces along normal directions and positions along tangent directions can be controlled. Each of these directions can be associated with a multiplier δ_i, (i=1…N)

$$\delta_i = \begin{cases} 1 & \textit{in position controlled direction} \\ 0 & \textit{in force controlled direction} \end{cases}$$

A selection matrix S can be defined as

$$\mathbf{S} = \begin{pmatrix} \delta_1 & 0 & \cdots & 0 \\ 0 & \delta_2 & \cdots & 0 \\ \vdots & \vdots & \ddots & \vdots \\ 0 & 0 & \cdots & \delta_N \end{pmatrix}. \tag{1}$$

The problem is to track predefined position trajectories and force trajectories (each in its own direction) by adjusting actuator torque based on output forces, positions, velocities and properties of the manipulator. There are two equations relating joint rates and joint torques with velocity and force of the end-effector.

$$\dot{\mathbf{q}} = \mathbf{J}^{-1}\dot{\mathbf{X}} \tag{2}$$

$$\boldsymbol{\tau} = \mathbf{J}^{\mathbf{T}}\mathbf{F} \tag{3}$$

In equations (2) and (3), **J** is the system Jacobian. The hybrid control scheme proposed by Raibert and Craig [3] is shown in Fig. 1. The control equation is given in Eq. (4).

$$\begin{aligned} \boldsymbol{\tau} = {} & \mathbf{J}^{\mathbf{T}}(\mathbf{G}+\mathbf{F}^{d}) + K_p[\mathbf{J}^{-1}((\mathbf{I}-\mathbf{S})\mathbf{X}_e) + c_1\mathbf{J}^{\mathbf{T}}(\mathbf{S}\mathbf{F}_e)] \\ & + K_d\mathbf{J}^{-1}(\mathbf{I}-\mathbf{S})\mathbf{V}_e + K_i\int[\mathbf{J}^{-1}((\mathbf{I}-\mathbf{S})\mathbf{X}_e) + c_2\mathbf{J}^{\mathbf{T}}(\mathbf{S}\mathbf{F}_e)]dt \end{aligned} \tag{4}$$

In hybrid control, the task space is divided into a force control subspace and position control subspace by the selection matrix. Though each degree of freedom is either in the force control loop or the position control loop, the actuators are adjusted based on the combined demands of position control and force control. In order to calculate the impact of force error and position error on the actuator, both Jacobian and inverse Jacobian are required. However, It is often the case that one of them is not easily available; generally, the inverse Jacobian is

difficult to obtain for a serial manipulator and the forward Jacobian is difficult to obtain for a parallel manipulator. In either case, inversion of Jacobian matrix becomes an inevitable step in the control process.

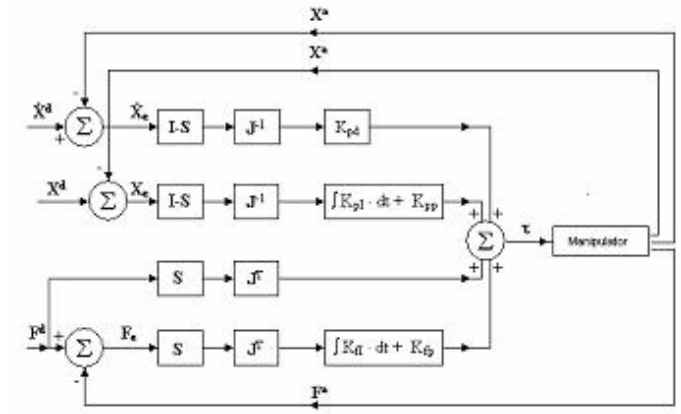

Figure 1: Original hybrid control scheme by Raibert and Craig.

Target tracking method developed in this paper aims at computational efficiency. Consider a case in which a manipulator is to be moved from a current configuration to a target configuration while the contact forces are changing to the desired values. Instead of feeding back force and position quantities through different controllers, the target tracking method either introduces an attractive force or velocity that is combined with other force or position quantities and fed through one controller. The attractive force or velocity is defined from the start configuration to the target configuration. This process is used to determine the joint torques.

In the case of serial manipulator forward Jacobian is easily obtained. Thus, it is desirable to define an attractive force from start position to target position because it would eliminate the need of Inverse Jacobian . The control scheme is depicted in Fig. 2.

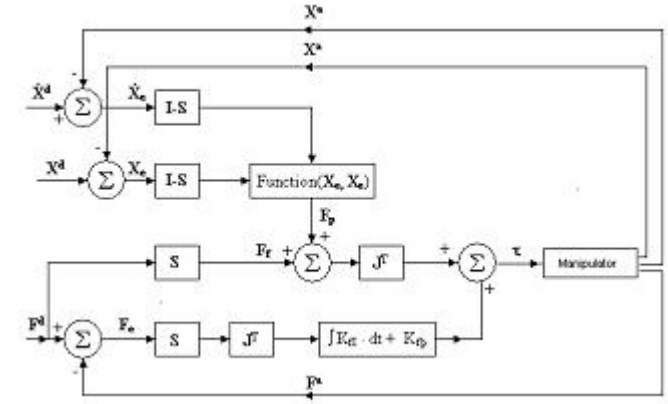

Figure 2: Target Tracking method for a serial manipulator.

The joint torque is calculated as

$$\boldsymbol{\tau} = \mathbf{J}^T[\mathbf{S}\mathbf{F}^d + (\mathbf{I}-\mathbf{S})(c_1\mathbf{X}_e + c_2\dot{\mathbf{X}}_e)] + K_p\mathbf{J}^T\mathbf{S}\mathbf{F}_e + K_i\int[\mathbf{J}^T\mathbf{S}\mathbf{F}_e]dt \quad (5)$$

The position errors are first converted into imaginary force quantities that are then combined with real force quantities on the other dimension of the task space to produce the input of the controller.

Alternately for a parallel manipulator, The inverse Jacobian is easily obtained, defining a velocity from the start position to the target position will eliminate the need of forward Jacobian. The control scheme is as depicted in Fig. 3. The Joint torque is calculated as

$$\boldsymbol{\tau} = K_p\mathbf{J}^{-1}[(\mathbf{I}-\mathbf{S})\mathbf{X}_e + c\mathbf{S}\mathbf{F}_e] + K_d\mathbf{J}^{-1}\mathbf{V}_e + K_i\int\mathbf{J}^{-1}[(\mathbf{I}-\mathbf{S})\mathbf{X}_e + c\mathbf{S}\mathbf{F}_e]dt \quad (6)$$

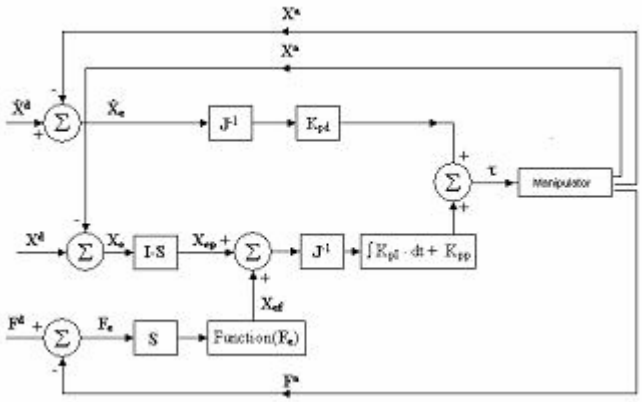

Figure 3: Target Tracking method for parallel manipulator.

The force errors are first converted into imaginary position quantities that are then combined with real position quantities on the other dimension of the task space to produce the input of the controller.

Compared to the Original Hybrid Control schema, in either case of Target Tracking method (serial or parallel manipulator), The inversion of system Jacobian matrix is replaced by a simple function and consequently improved the computation efficiency. For a general n by n square matrix, The inversion calculation requires a computational complexity of $O(n^3)$ [19,20] and usually results in the biggest computation burden in the programming of control cycles.

TARGET TRACKING THEORY IN AN OPEN LOOP MANIPULATOR (3-DOF CASE STUDY)

In this section, we will study a simulation of a simple open loop manipulator consisting of a series of 3 links connected to

each other in a series and to ground by revolute joints. A torque-controlled motor is attached to each joint. The simulation is constructed in Working Model 5 by MSC Software, and the control is implemented using Matlab 6.5. If the task is to control position, a constant hand velocity of 0.4m/s is defined while keeping the hand orientation horizontal or at an angle of $\pi/3$ radians relative to the wall (see Table 1 for more detail). If the task is to control contact force against a rigid wall, a force of 10N is used in the directions depicted below. Cases are studied on a flat wall, on a wall with a ramp disturbance, and with a time varying force disturbance. Excluding the first two simulations, hybrid and target tracking manipulation theories are used for each case (refer to Table 1).

Table 1: Representations of 2D simulations performed in Working Model.

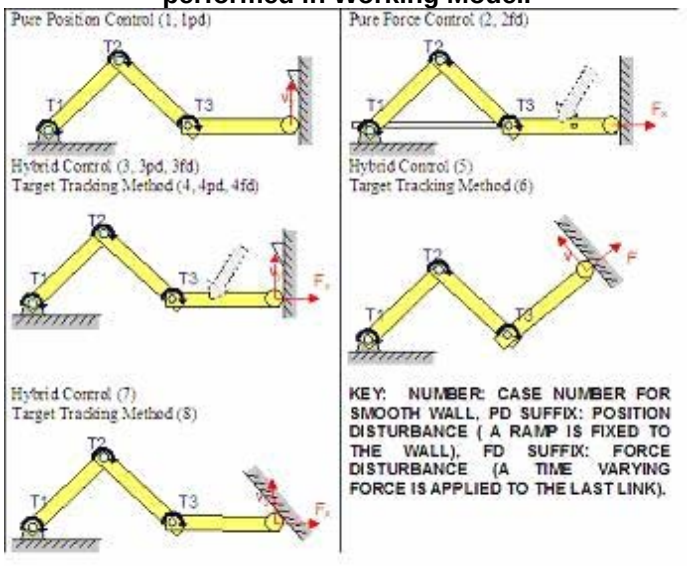

Table 2: Error comparison between manipulation methods for 2D simulations.

Case Number	Manipulation Method	Force Error Function	Position Error Function
1	Position Control	0	156.4
1pd	Position Control	0	612.5
2	Force Control	656.8	0
2fd	Force Control	2638	0
3	Hybrid Control	2409	124.7
4	Target Tracking	873.5	0.3463
3pd	Hybrid Control	6009	151.6
4pd	Target Tracking	3856	0.9487
3fd	Hybrid Control	5157	200.2
4fd	Target Tracking	3453	0.4684
5	Hybrid Control	3665	274.0
6	Target Tracking	2771	0.3489
7	Hybrid Control	17740	4795
8	Target Tracking	2539	3.301

An objective error function was defined for the simulations as the sum of the magnitude of the error vector over a given time interval. These values are presented below in Table 2.

In all cases, the force and position error are significantly reduced by using the target tracking manipulation technique. The position error is reduced in the cases with and without the position disturbance (for the smooth and bumped wall). In the target tracking scheme, the successful control of position is the primary concern because inverse kinematics is not being used. The manipulation theory proves to be stable and successful in these 2D simulations.

It should be noted that in these simulations gains for the controllers have not been optimized. The gains are unaltered in each simulation using hybrid and target tracking control schemes. So the gains in the force control part of the hybrid scheme are used in the target tracking scheme. These would need to be optimized to reduce the settling time and other error characteristics for each scheme, but by using the same gains in each force controller, a general comparison can be made without the influence of the controller gains.

Next, the results of one particular simulation are presented. The setup is shown above in cases 3 and 4 (for hybrid control and target tracking respectively). The wall is smooth and the desired force is 10N, but the desired velocity is not constant. The position is defined below:

$$\theta = 0, \qquad x = x_{0,}$$

$$y = \begin{cases} y_0 + 0.2\left(1 + \sin\left(\frac{\pi}{4}t - \frac{\pi}{2}\right)\right) & \text{for } t \le 12 \\ y_0 + 0.4 & \text{for } t > 12 \end{cases}$$

As defined, the manipulator will press against a wall and oscillate for the first 12 seconds as in a grinding process. Then the manipulator will stop, while maintaining the 10N force. The results are shown in Fig. 1 and tabulated in Table 3 for hybrid control (HC) and target tracking (TT).

Table 3: Simulation error function results.

Method	Force Error Function	Position Error Function
Hybrid Control (HC)	2198	58.22
Target Tracking (TT)	970.0	0.4402

As the results of this simulation suggest, the target tracking method has an advantage of not only reducing the error function, but also eliminates the burden of computing the inverse Jacobian thus reducing the computational complexity.

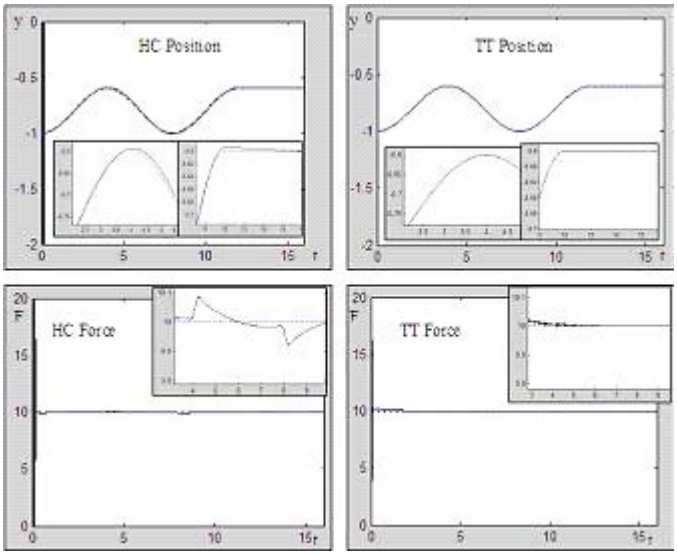

Figure 4: Simulation results

TARGET TRACKING THEORY IN AN OPEN LOOP MANIPULATOR: APPLICATION ON A PUMA

In the mid-1970's, Victor Scheinman developed a PUMA (Programmable Universal Machine for Assembly) manipulator. A general PUMA manipulator (see Fig. 5) has six serial links connected to each other and ground by revolute joints. The joints are actuated by motors to move the hand in the workspace. An assortment of tools can be attached to the hand of the manipulator for various tasks.

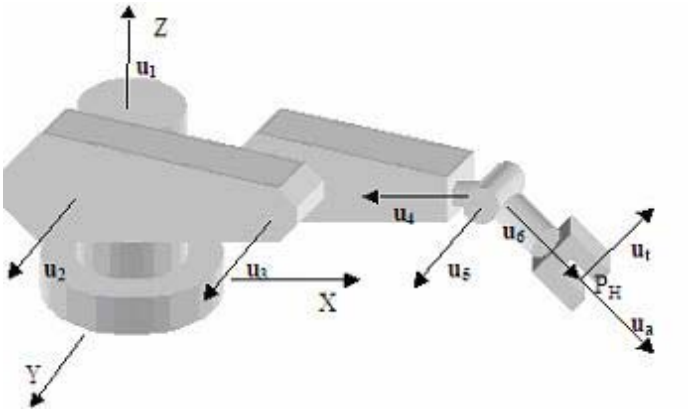

Figure 5: A general PUMA manipulator.

There are two fundamental problems in manipulator kinematics, direct kinematics and inverse kinematics. Direct kinematics is the process of transforming the joint coordinates, joint rates, and joint accelerations into position, velocity, and acceleration of the end-effector. Alternately, inverse kinematics calculates joint parameters in terms of the end-effector parameters. The solution of the forward kinematics of the puma manipulator is straightforward. On the other hand, the inverse kinematics is extremely complicated and involves solving a set of highly nonlinear, coupled equations. This problem is even more difficult if the manipulator is in a singular configuration.

The Jacobian of the serial manipulator is calculated using zero-position notation [18]. Referring to Eq. (2), the definition of the Jacobian is

$$\dot{\mathbf{x}}_{\mathbf{H}} = \mathbf{J}\dot{\mathbf{q}}, \tag{7}$$

where $\dot{q}$ is the vector of joint rates and $\dot{x}_{\mathbf{H}} = [\boldsymbol{\omega}_{\mathbf{H}} \mid \mathbf{v}_{\mathbf{H}}]^T$. The forward kinematics can be performed by determining the hand velocity relative to the base coordinate system. This results in the following

$$\begin{pmatrix} \boldsymbol{\omega}_{\mathbf{H}} \\ - \\ \mathbf{v}_{\mathbf{H}} \end{pmatrix} = \begin{pmatrix} u_1 & \cdots & u_6 \\ \vdots & \ddots & \vdots \\ u_1 \times P_1^2 h & \cdots & u_6 \times P_6^7 h \end{pmatrix} \begin{pmatrix} \dot{q}_1 \\ \vdots \\ \dot{q}_6 \end{pmatrix}, \tag{8}$$

where $P_j^{j+1}h = \sum_{k=j+1}^{7} b_k$ and b_k is the body vector from joint k to k+1 in the current configuration. Hence the Jacobian is just

$$\mathbf{J} = \begin{pmatrix} u_1 & \cdots & u_6 \\ \vdots & \ddots & \vdots \\ u_1 \times P_1^2 h & \cdots & u_6 \times P_6^7 h \end{pmatrix}. \tag{9}$$

Similarly, a relation between force at the hand and the joint torques can be derived. It is rewritten from Eq. (3) as

$$\begin{pmatrix} \tau_1 \\ \vdots \\ \tau_6 \end{pmatrix} = \mathbf{J}^T \begin{pmatrix} \mathbf{M}_{\mathbf{H}} \\ - \\ \mathbf{F}_{\mathbf{H}} \end{pmatrix}. \tag{10}$$

In typical hybrid control Eqs. (2) and (10) are used for the position and force control loops, respectively.

Case Study

In the following section, the target tracking method will be used in a 3-Dimensional example. A PUMA manipulator having the characteristics listed in Table 4 is simulated in Matlab. A wall is simulated by applying a force only in the x-direction at the hand of the manipulator when the hand moves beyond a specified coordinate in the x-axis. The value of the force is dependant on the geometry of the tool and wall. To simulate this force the PISE method is used [21]. The desired force is 10N, and the desired position is in the z-direction and is a function of time (12 seconds of a sinusoidal motion followed by 3 seconds at a constant position).

Table 4: PUMA Properties

Link	1	2	3	4	5	6
Body Vector	0 10 0	17 0 0	0 0 -17	0 0 0	0 0 0	0 0 -5
Joint to CG	0 5 0	8 2 0	0 0 -9	0 0 -1	0 -1 0	0 0 -3
Joint Axis	0 0 1	0 1 0	0 1 0	0 0 1	0 -1 0	0 0 -1
Weight	10	16	12	1	1	6
Moment of Inertia [Ixx Iyy Izz]	.230 .005 .230	.069 1.453 1.394	1.405 1.585 0.034	.001 .001 .0001	.001 .0001 .001	.069 .069 0.01

In the plots that follow, the dashed line is the desired value, while the solid line is the actual value. Force and position are shown only in the direction containing the desired motion or force. Two simulations are shown.

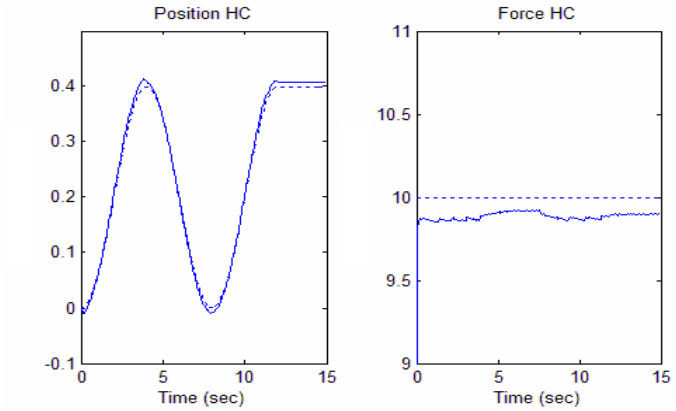

Figure 6: Hybrid Control [Kp=6e3; Ki=3e2; Kd=4e2; c_1=1.67e-2; c_2=3.33e-3]

Fig. 6 is the typical hybrid control, followed by the target tracking scheme in Fig. 7. Errors are displayed in Table 5. For this case, target tracking has less error while maintaining a constant force during the process. In fact, one cannot differentiate the dashed from solid line in the position plot of Fig. 7. Note that with these gains, the force control feedback gains remain constant for both simulations. A better position accuracy can be achieved by increasing the dependance of the attractive force on the position error.

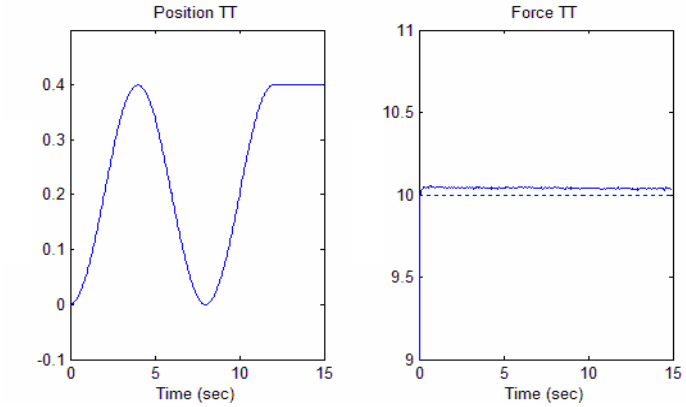

Figure 7: Target Tracking [Kp=1e2; Ki=1; Kd=2e-1; c_1=2e3; c_2=1e1]

Table 5: Simulation error function results.

Error Functions	Hybrid Control (HC)	Target Tracking (TT)
Sum of X_e in z-direction (Cumulative Position Error)	8.4	1.6e-4
Sum of F_e in x-direction (Cumulative Force Error)	2.4e3	7.2e2

TARGET TRACKING THEORY IN A CLOSED LOOP MANIPULATOR: APPLICATION ON A STEWART PLATFORM

The Stewart Platform is a popular six DOF parallel manipulator. It was first introduced by Stewart as an airplane simulator [22]. The general SP consists of a base link, a coupler link and six chains connected in parallel between the base and the coupler. Each chain consists of a prismatic (sliding) joint with a ball-joint connection to the base and the coupler. Each of the prismatic joints serves as an independent input. Stewart Platform has the advantages of simplicity, high stiffness, large load capacity, quick dynamic response and good accuracy.

As previously stated, there are two fundamental problems in manipulator kinematics, direct kinematics and inverse kinematics. In contrast to the serial manipulator, the inverse kinematics of the Stewart Platform is easy to solve. However, the forward kinematics is extremely complicated and involves solving a set of highly nonlinear and coupled equations. The following is a kinematic analysis of the Stewart Platform. Figure 8 represents Stewart platform of the most general geometry.

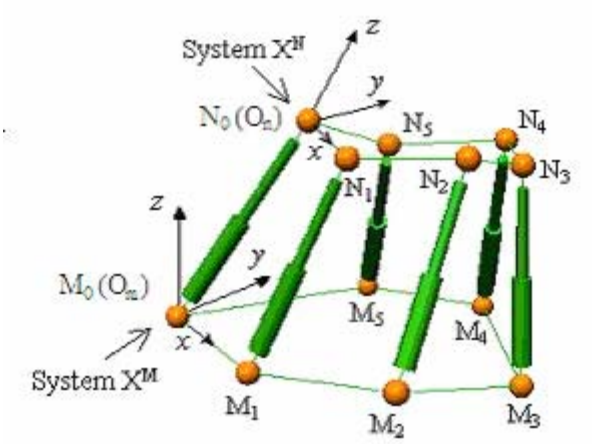

Figure 8: Stewart Platform of General Geometry

Coordinate $O_m(x_m\text{-}y_m\text{-}z_m)$ is rigid to the base platform. Coordinate system $O_n(x_n\text{-}y_n\text{-}z_n)$ is rigid to the mobile platform. Six limbs are connected at six distinct points N_i on coupler platform and M_i on the base platform (i=0...5. In this paper, unless denoted specifically, index i ranges from 0 to 5). It can be observed that the configuration of the platform is completely determined by the lengths of the 6 limbs l_i, i.e. the distance M_i N_i. Cartesian coordinate system O^N is fixed to the coupler platform, whereas O^M is fixed to the base platform. The coordinates of points M_i, N_i are known in O^M and O^N respectively. Let $N_i^N = (n^N_{ix}, n^N_{iy}, n^N_{iz})^T$, $M_i^M = (m^M_{ix}, m^M_{iy}, m^M_{iz})^T$, where the superscripts M and N denote the reference coordinate systems.

In Figure 8, we observe that:

$$\begin{aligned}\underline{M_iN_i}^M &= \underline{O_mO_n} + \underline{O_nN_i} - \underline{O_mM_i} \\ &= \mathbf{p} + \mathbf{R}\cdot\underline{O_nN_i}^N - \underline{O_mM_i}^M \quad (k=0\ldots5)\end{aligned} \tag{11}$$

Where $\underline{O_mO_n}^M = \mathbf{p}$ describes the position of the origin of the end-effector coordinate system as the reference point with respect to the base coordinate system. $\mathbf{R} = \mathbf{R}_{0,n} = (\mathbf{u} \quad \mathbf{v} \quad \mathbf{w})$ is the rotation matrix from the base coordinate system to the end-effector system, witch can be defined with the three Euler's angles Denote the values of the six prismatic values to be q_i, take inner product of both sides of Eq. (11), we have:

$$\begin{aligned}q_i^2 &= \underline{M_iN_i}\cdot\underline{M_iN_i} \\ &= (\mathbf{p} + \mathbf{R}\cdot\underline{O_nN_i}^N - \underline{O_mM_i}^M)\cdot(\mathbf{p} + \mathbf{R}\cdot\underline{O_nN_i}^N - \underline{O_mM_i}^M) \\ &= \mathbf{p}\cdot\mathbf{p} + 2\cdot\mathbf{p}\cdot(\mathbf{R}\cdot\underline{O_nN_i}^N) - 2\cdot\underline{O_mM_i}^M\cdot(\mathbf{R}\cdot\underline{O_nN_i}^N) - 2\cdot\mathbf{p}\cdot\underline{O_mM_i}^M \\ &\quad + \underline{O_mM_i}^M\cdot\underline{O_mM_i}^M + \underline{O_nN_i}^N\cdot\underline{O_nN_i}^N\end{aligned} \tag{12}$$

The joint values of the 6 prismatic joints depend uniquely on the posture of the Stewart Platform. The direction vector of limb I is calculated by Eq. (11) its length can be calculated directly from Eq. (12) by taking square root of both sides:

$$q_k = (\mathbf{p}\cdot\mathbf{p} + 2\cdot\mathbf{p}\cdot(\mathbf{R}\cdot\underline{O_nN_i}^N) - 2\cdot\underline{O_mM_i}^M\cdot(\mathbf{R}\cdot\underline{O_nN_i}^N) - 2\cdot\mathbf{p}\cdot\underline{O_mM_i}^M + \underline{O_mM_i}^M\cdot\underline{O_mM_i}^M + \underline{O_nN_i}^N\cdot\underline{O_nN_i}^N)^{1/2} \tag{13}$$

As with the position mapping problem, the velocity mapping between actuator and end-effector coordinates is more easily found as the inverse map, from the end-effector velocities to limb velocities, and we define the inverse Jacobian $\mathbf{J}^{-1}$ by:

$$\dot{\mathbf{q}} = \mathbf{J}^{-1}\cdot\dot{\mathbf{x}} \tag{14}$$

where $\dot{\mathbf{q}}$ is the vector of limb joint rates, and $\dot{\mathbf{x}} = (\boldsymbol{\omega} \mid \dot{\mathbf{p}})^T$ is the velocity of the velocity of the end-effector consisting of translation and rotation components. Let $\mathbf{w_i}$ be the unit vector along $\underline{M_iN_i}$, Differentiating Eq. (11) yields:

$$\dot{q}_i\,\mathbf{w_i} + q_i\,\dot{\mathbf{w}}_i = \dot{\mathbf{p}} + (\boldsymbol{\omega}\times\underline{O_nN_i}) \tag{15}$$

Since $\mathbf{w_i}$ is a unit vector, $\mathbf{w_i}\cdot\mathbf{w_i}=1$, $\mathbf{w_i}\cdot(d\mathbf{w_i}/dt)=0$, Thus, taking the inner product of $\mathbf{w_i}$ on both sides of (15) yields:

$$\begin{aligned}\dot{q}_i &= \mathbf{w_i}\cdot\dot{\mathbf{p}} + \mathbf{w_i}\cdot(\boldsymbol{\omega}\times\underline{O_nN_i}) \\ &= \mathbf{w_i}\cdot\dot{\mathbf{p}} + (\underline{O_nN_i}\times\mathbf{w_i})\cdot\boldsymbol{\omega}\end{aligned} \tag{16}$$

Equation 16 reflects the relation between joint rates and end-effector velocities. Rewrite it in the format of matrix

$$\dot{\mathbf{q}} = \begin{pmatrix} \underline{O_nN_0}\times\mathbf{w}_0 & \mathbf{w}_0^T \\ \vdots & \vdots \\ \underline{O_nN_5}\times\mathbf{w}_5 & \mathbf{w}_5^T \end{pmatrix}\cdot\begin{pmatrix}\boldsymbol{\omega} \\ \dot{\mathbf{p}}\end{pmatrix} \tag{17}$$

the inverse Jacobian is given by

$$\mathbf{J}^{-1} = \begin{pmatrix} \underline{O_nN_0}\times\mathbf{w}_0 & \mathbf{w}_0^T \\ \vdots & \vdots \\ \underline{O_nN_5}\times\mathbf{w}_5 & \mathbf{w}_5^T \end{pmatrix} \tag{18}$$

As illustrated above, the inverse kinematics of Stewart Platform is quite trivial, However the forward kinematics of Stewart Platform is very complicated. After solutions for some special cases were discovered [23,24,25,26,27,28,29,30,31,32], Husty derived a closed-form solution of 40 degree polynomial equation for the most general Stewart platform [33]. Mu and Kazerounian developed a numerical method to look for all 40 solutions efficiently [34]. However, considering time efficiency, all of these direct kinematic solutions involved numerical root finding process for polynomial equations and are not suitable for being used in a real-time target tracking control.

Case study

In this section we demonstrate the target tracking algorithm on a Stewart Platform that has the following properties: The six points M_i (i=0…5), which connect legs with

the base platform, are in plane x_m-O_m-y_m. M_0, M_2, M_4 coincide with M_1, M_3 and M_5 respectively. There is one prismatic joint (referred as top joint) in plan x_n-O_n-y_n. Six prismatic joints (referred as leg joints) M_0N_0, M_1N_1, M_2N_2, M_3N_3, M_4N_4, and M_5N_5 connect the base platform at $M_{0\sim1}$, $M_{2\sim3}$, $M_{4\sim5}$. The position of M_i and N_i in System O_m and O_n are specified by the distance of O_mM_i and O_nN_i and their angles with respect to axis x_m and x_n. O_n N_0 is actually the joint value of q_{01}. They are given in the following tables,

Table 6: Position of Ni

I	0	1	2	3	4	5
O_nN_I	0.7	0.7	0.7	0.7	0.7	0.7
$\angle$ $X_nO_nN_i$	-π/6	Π/6	π/2	5π/6	7π/6	3π/2

Table 7: Position of Mi

I	0	1	2	3	4	5
O_nM_i	1.0	1.0	1.0	1.0	1.0	1.0
$\angle$ $X_mO_mM_i$	0	0	2π/3	2π/3	4π/3	4π/3

The end-effector of the Stewart platform is mounted at the center O_n of the mobile platform, Denote it with H (coincided with O_n). The Stewart Platform is expected to move H along a sine trajectory for 12 seconds. The end-effector is in contact with a planar surface P. Denote time with t ($8\geq t\geq 0$), In O_m system, Define end-effector's actual position $\mathbf{X^a}$=(X^a, Y^a, Z^a, θ^a, Φ^a, Ψ^a)^T where θ^a, Φ^a, Ψ^a are the XYZ Euler angle of coordinate system $O_n(x_n$-y_n-$z_n)$ with respect to coordinate system $O_m(x_m$-y_m-$z_m)$; actual velocity $\mathbf{V^a}$=(V_x^a, V_y^a, V_z^a, ω_x^a, ω_y^a, ω_z^a)^T; actual contact force $\mathbf{F^a}$=(F_x^a, F_y^a, F_z^a, T_x^a, T_y^a, T_z^a)^T; desired position $\mathbf{X^d}$=(X^d, Y^d, Z^d, θ^d, Φ^d, Ψ^d); desired velocity $\mathbf{V^d}$=(V_x^d, V_y^d, V_z^d, ω_x^d, ω_y^d, ω_z^d)^T; desired contact force $\mathbf{F^d}$=(T^d_x, T^d_y, T^d_z, F^d_x, F^d_y, F^d_z)^T; the trajectory is described as:

$$\begin{cases}\mathbf{X}^d = (\theta^d, \phi^d, \psi^d, x^d, y^d, z^d)^T = (0, 0, 0, 0.2\cdot[1+\sin(t\cdot\pi/4)], 0, z^a)^T \\ \mathbf{F}^d = (T_x^d, T_y^d, T_z^d, F_x^a, F_y^a, F_z^a) = (T_x^a, T_y^a, T_z^a, F_x^a, F_y^a, 10)\end{cases}$$

During the motion, x, y position and orientation of the end-effector are controlled, but position in z direction is not controlled, it is just equal to Z^a. Similarly, the contact force in z direction at the between end-effector and plan P is controlled to be F^d, but F_x, F_y, T_x, T_y, T_z are not controlled. At t=0, H is at position (0, 0, 1); θ=0 , Φ =0, Ψ=0. Assume that there is no friction on the surface P, and that P only generates a reaction force in the negative z_m direction. The task is simulated with software package Matlab 6.5 and VisualNastran 4D. In the experiment, the real reaction force F_z^a of plan P is simulated according to F_z^a= -100(z^a-1).

The joint torques are calculated by Eq. (6). All feedback gains and constants are chosen empirically to provide stable and accurate control. The detailed calculation steps are listed in appendix.

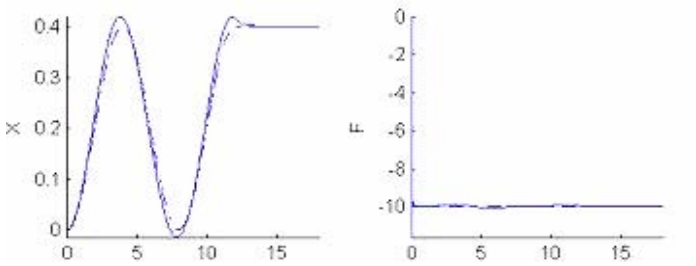

Figure 9: Position and force trajectories with Target Tracking method

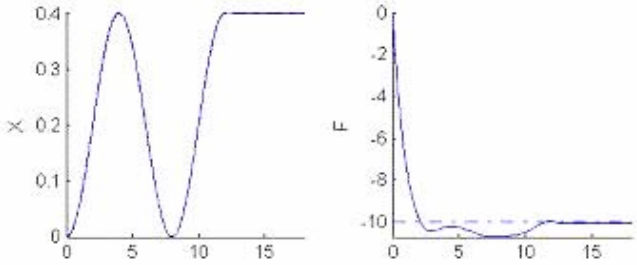

Figure 10: Position and force errors Hybrid Control

Figures 9 and 10 showed the position and force trajectories of the simulation result with the target tracking method and Hybrid Control respectively. In either case, the end-effector follow both desired force trajectory and position trajectory smoothly. all errors are with accuracy tolerance . The following table displays error function results in all six dimensions.

Table 8: Simulation error function results.

Method	Hybrid Control (HC)	Target Tracking (TT)
Sum of x_e	5.0984	44.6526
Sum of y_e	0	0
Sum of F_e	2.3428	174.4670
Sum of ϕ_e	0	0
Sum of θ_e	0.0012	11.0496
Sum of Ψ_e	0	0

CONCLUSION

A target tracking manipulation method is developed which realized hybrid position/force control of robotic manipulator without requirements of solution of both direct kinematics and inverse kinematics. In serial manipulators, the direct kinematics is easy to solve but the inverse kinematics is generally difficult. In parallel manipulators, the reverse is true. For a compliant motion task with a serial manipulator, virtual forces are applied in the direction of position errors and converted into joint torque space only through the forward system Jacobian. Similarly, for a compliant motion task with parallel manipulator, virtual position errors are constructed to replace

the force error and converted into joint torque space only through the inverse system Jacobian. The computational burden is reduced significantly since the inversion of the Jacobian matrix is eliminated. The strategies for applying the virtual force or virtual motion are independent of the control scheme and can be designed separately. This method inherited the conceptual simplicity of hybrid control [3] to satisfy both position and force constraints simultaneously. In the position/force tracking process, only the kineto-static model is required and no dynamic calculations are involved. Simulation experiments are presented to demonstrate the application of this method on a serial and parallel manipulator. The results show the tracking processes are accurate and stable along both position trajectory and force trajectory.

ACKNOWLEDGMENTS

The first author wishes to acknowledge the NSF Fellowship (under contract NSF-0139307) that supports the Galileo Program at the University of Connecticut.

REFERENCES

1. Paul, R. and Shimano, B., 1976, “Compliance and Control”, *Joint Automatic Control Conference*, Sanfrancisco, LA.
2. Mason, M. T., 1981, “Compliance and Force Control for Computer-Controlled Manipulators”, *IEEE Transactions on Systems, Man and Cybernetics*, Vol.SMC-11, No. 6.
3. Raibert, M.. H. and Craig, J. J., 1981, “Hybrid Position/Force Control of Manipulators”, *ASME Journal of Dynamic Systems, Measurement and Control*, Vol. 102, pp. 126-133, June.
4. Zhang, H. and Paul, R. P., “Hybrid Control of Robotic Manipulators”, *International Conference on Robotics and Automation*, IEEE Computer Society, pp. 602-607, Sant Louis, Missouri, March 1985.
5. Liu, J. and Chen, S., 1998, “Robust Hybrid Control of Constrainted Robot Manipulators via Decomposed Equations”, *Journal of Intelligent and Robotic Systems”*, Vol. 23, pp. 45-70.
6. Duffy, J., 1990 “The Fallacy of Modern Hybrid Control Theory That is Based on ‘Orthogonal Complements’ of Twist and Wrench Spaces”, *Journal of Robotic Systems*, Vol. 7, pp. 139-144.
7. Zhang, M. H., “Kinematic Stability of Robot Manipulators under Force Control”, *International Conference on Robotics and Automation*, IEEE Robotics and Automation Society, pp. 80-85, Scottsdale, Arizona, May 1989.
8. Fisher, W. D. and Mujtaba, S. M., 1991, “Hybrid Position/Force Control: A Correct Formulation”, Lab Report HPL-91-140, Measurement and Manufacturing Systems Laboratory, Hewlett-Packard Company, Cot.
9. Khatib, O., Featherstone, R., Thiebaut, S., 1999, “A General Contact Model for Dynamically-Decoupled Force/Motion Control”, Proc. Of 1999 IEEE International Conference on Robotics and Automation. May 10-15, 1999, Detroit, MI, Paper No. 0-7803-5180-0-5/99.
10. Hogan, N., 1985, “Impedance Control: An Approach to Manipulation:Part I-Theory”, *Transaction of the ASME, Journal of Dynamic Systems, Measurement and Control*, Vol. 107, pp. 1-7, March.
11. Hogan, N., 1985, “Impedance Control: An Approach to Manipulation:Part II-Implementation”, *Transaction of the ASME, Journal of Dynamic Systems, Measurement and Control*, Vol. 107, pp. 8-16, March.
12. Hogan, N., 1985, “Impedance Control: An Approach to Manipulation:Part III-Application”, *Transaction of the ASME, Journal of Dynamic Systems, Measurement and Control*, Vol. 107, pp. 17-24, March.
13. Maples, J. and Becker, J., 1986, “Experiments in Force Control of Robotic Manipulators”, *Proceedings of IEEE international Conference on Robotics and Automation*, pp. 695-702.
14. Kazerooni, H., 1987, “Robust, Non-Linear Impedance Control for Robot Manipulators", *Proceedings of the IEEE International Conference on Robotics and Automation*, pp. 741-750.
15. Wen, J. T. and Murphy, S., 1991, “Stability analysis of position and force control for robot arms”, *IEEE Transaction on Automation and Control*, Vol. 36, pp. 365–371, March.
16. Waibel, B. and Kazerooni, E., 1991, “Theory and experiment on the stability of robot compliance control,” *IEEE Trans. Robot. Automat.*, vol. 7, pp.95–104, June.
17. Walker, I.D., 1990, “The Use of Kinematic Redundancy in Reducing Impact and Contact Effects in Manipulation", *Proceedings of the IEEE International Conference on Robotics and Automation*, pp. 434-439.
18. Kazerounian, K. and Gupta, K. C., 1984, “A Target Tracking Manipulation Theory for Robots”
19. Westlake, J. R. 1968, “A hand book of Numerical Matrix Inversion and Solution of Linear Equations, Wiley inc, New York.
20. Press W. H., Teukolsky, S. A. Vetterling, W. T. and Flannery, B. P. 1992, “Numerical Recipes in C”, Cambridge University Press, Cambridge, UK.
21. Pimsarn, M. and Kazerounian, K., 2003, “Pseudo-interference stiffness estimation, a highly efficient numerical method for force evaluation in contact problems”, *Engineering with Computers*, Vol. 19, pp. 85-91.
22. Stewart, D., 1965, "A Platform with Six Degree of Freedom", *Proc. Inst. Mech. Eng.*, London, Vol. 180, pp. 371-386.
23. Kohli, D. Lee, S.H., Tsai K. Y. and Sandor, G. N., 1988, "Manipulator Configurations Based on Rotary-Linear(R-L) Actuators and Their Direct and Inverse Kinematics",

ASME Journal of Mechanisms. Transmissions, and Automation in Design, Vol. 110, pp. 397-404, Dec.
24. Griffis, M and Duffy J., 1989, "A Forward Displacement Analysis of a Class of Stewart Platforms", *Journal of Robotic Systems*, Vol. 6, No.6, pp. 703-720.
25. Innocenti, C., and Parenti-Castelli, V., 1990, "Direct Position Analysis of the Stewart Platform Mechanism", *Mechanism and Machine Theory*,Vol. 25, No. 6, pp. 611-621.
26. Innocenti, C. and Parenti- Castelli, V., 1993, "Closed-Form Direct Position Analysis of a 5-5 Parallel Mechanism", *Journal of Mechanical Design*, Vol. 115, pp. 515-521, Sept.
27. Chen, N. X. and Sing, S. M., 1994, "Direct Position Analysis of the 4-6 Stewart Platform", *Journal of Mechanical Design*, Vol. 116, pp. 61-66, March.
28. Zhang, C. D. and Song, S. M., 1992, "Forward Kinematics of a class of Parallel (Stewart) Platforms with closed form Solutions", *Journal of Robotic Syste*ms, Vol. 9, No. 1, pp. 93-112, Jan.
29. Zhang, C. D. and Song, S. M., 1994, "Forward Position Analysis of Nearly General Stewart Platforms", *Journal of Mechanical Design*, Vol. 116, pp. 54-60, March.
30. Lin, W. , Grane, C. D. and Duffy, J., 1994, "Closed Form Forward Displacement Analysis of the 4-5 in Parallel Platforms", *ASME J. Mech. Design*, Vol. 116, pp. 47-53.
31. Nanua, P. Waldron, K. J. and Murphy, V., 1990, "Direct Kinematic Solution of a Stewart Platform", *IEEE Transactions on Robotics and Automation*, Vol. 6, No. 4, pp. 438-444.
32. Lee, J. K. and Song, S. M., 1990, "A Study of Instantaneous Kinematics of walking machines", *International Journal of Robotic Systems*, Vol. 9, No. 1, pp. 93-112, Jan.
33. Husty, M. L., 1996, "An Algorithm for Solving the Direct Kinematics of General Stewart-Gough Platforms", Mechanism and Machin Theory, Vol. 31, No. 4, pp. 365-380.
34. Mu, Z. and Kazerounian, K, 2002, "A Real Parameter Continuation Method for Complete Solution of Forward Position Analysis of the General Stewart", *ASME Journal of Mechanical Design*.
35. Craig, J. J. and Raibert, M. H., "Asystematic Method for Hybrid Position/Force Control of a Manipulator", *Proc. 1979 IEEE Computer Software Application Conference*, Chicago, Ill, Nov. 6-8, 1979.
36. Innocenti, C., 1998, "Forward Kinematics in Polynomial Form of the General Stewart Platform", Proc. Of 1998 ASME Design Engineering Technical Conferences. Sept. 13-16, 1998, Atlanta, GA, Paper No. DETC98/MECH-5894.
37. Khatib, O., 1987, "A Unified Approach for Motion and Force Control of Robotic Manipulators: The Operational Space Formulation", IEEE transaction on Robotic and Automation, Vol. 3, pp: 43-53.

APPENDIX

In the experiment of the target tracking of Stewart Platform, the joint torque is calculated by

$$\boldsymbol{\tau} = K_p \cdot \mathbf{J}^{-1} \cdot [\mathbf{S} \cdot \mathbf{X}_e + c_F \cdot (\mathbf{I} - \mathbf{S}) \cdot \mathbf{F}_e] + K_d \cdot \mathbf{J}^{-1} \cdot \mathbf{V}_e + \int K_I \cdot \mathbf{J}^{-1} \cdot [\mathbf{S} \cdot \mathbf{X}_e + c_F \cdot (\mathbf{I} - \mathbf{S}) \cdot \mathbf{F}_e] \cdot dt$$

The integral, KI=1 Nm/ Kp=100, Kd=10,C_F= -0.05.
S is the selection matrix,

$$\mathbf{S} = \begin{pmatrix} 100000 \\ 010000 \\ 000000 \\ 000100 \\ 000010 \\ 000001 \end{pmatrix}.$$

Then force error is: $\mathbf{F_e}=\mathbf{F^d}-\mathbf{F^a}$
Velocity error is: $\mathbf{V_e}=\mathbf{V^d}-\mathbf{V^a}$
Position error is calculated as follows:
Displacement error:

$$\Delta\mathbf{Pos}=(X^d-X^a,\ Y^d-Y^a,\ Z^d-Z^a)^T$$

Angular error:

$$\Delta\mathbf{Ang}=(\theta^d-\theta^a,\ \Phi^d-\Phi^a,\ \Psi^d-\Psi^a)^T$$

B matrix for XYZ Euler angle is:

$$\mathbf{B} = \begin{pmatrix} 1 & 0 & \sin(\phi) \\ 0 & \cos(\theta) & -\sin(\theta)\cdot\cos(\phi) \\ 0 & \sin(\theta) & \cos(\theta)\cdot\cos(\phi) \end{pmatrix}$$

Let $\Delta Ang' = C_A \cdot \mathbf{B} \cdot \Delta Ang$, C_A is the scaling factor for angular quantities. Then:

$$\mathbf{X}_\mathbf{e} = \begin{pmatrix} \Delta Pos \\ \Delta Ang' \end{pmatrix} = \begin{pmatrix} \Delta Pos \\ \mathbf{B} \cdot \Delta Ang \end{pmatrix}$$